

Advantages of Monochromatic X-rays for Imaging

M. Hoheisel¹, R. Lawaczeck², H. Pietsch², and V. Arkadiev³

¹ Siemens AG Medical Solutions, Forchheim, Germany

² Schering AG Diagnostics and Radiopharmaceuticals Research, Berlin, Germany

³ IAP - Institut für Angewandte Photonik e.V. and IfG - Institute for Scientific Instruments GmbH, Berlin, Germany

ABSTRACT

The contrast of X-ray imaging depends on the radiation energy and acquires its maximum value at a certain optimum energy typical for the object under investigation. Usually, higher energies result in reduced contrast, lower energies are absorbed in the object thus having a smaller probability of reaching the detector. Therefore, broad X-ray spectra contain non-optimal quanta to a large extent and deliver images with deteriorated contrast.

Since investigations with monochromatic X-rays using synchrotrons are too complex and expensive for routine diagnostic imaging procedures, we propose a simpler approach. A conventional mammography system (Siemens Mammomat[®] 300) with an X-ray tube with a molybdenum anode was supplemented with an X-ray HOPG monochromator (HOPG = Highly Oriented Pyrolytic Graphite) and an exit slit selecting those rays fulfilling Bragg's condition. The detector is a CCD (Thales TH9570), 4092×200 pixels, $54 \mu\text{m}$ in size. At this slot-scan setup¹, measurements have been carried out at 17.5 keV as well as with a polychromatic spectrum with 35 kV tube voltage.

The modulation transfer function (MTF) and the detective quantum efficiency (DQE) have been determined from images of a lead bar pattern and flat-field images. Both MTF and DQE depend on orientation (scan or detector direction) for the 17.5 keV monochromatic case. Above 3 mm^{-1} the DQE values are smaller than those for polychromatic radiation.

The contrast yielded by foils of different materials (Al, Cu, Y, Ag) has been studied. In all cases the monochromatic X-rays give rise to about twice the contrast of a polychromatic spectrum.

Keywords: X-ray imaging, monochromator, HOPG, modulation transfer function, detective quantum efficiency, contrast media

1. INTRODUCTION

In the field of medical X-ray imaging, much effort has been directed towards finding an optimum spectrum for every specific diagnostic situation. This includes the choice of the anode material of the X-ray tube, the tube voltage, as well as the material and thickness of additional filters².

To visualize a certain lesion, the ratio of contrast to noise should be as high as possible, where contrast means the signal difference between lesion and surrounding tissue. Since the absorption coefficient becomes smaller with increasing energy, low energy will deliver high contrast. Unfortunately, with lower energy, the patient dose increases while more quanta are absorbed in the object and less quanta will reach the detector and be registered. So there must be an optimum energy in between. This gives rise to the demand for a monochromatic X-ray source working at this very energy. A simulation study on this subject has been conducted by Boone and Seibert among others³.

Up to now, monochromatic X-rays have been produced by synchrotrons, which is a very expensive and complex method. Therefore, synchrotron radiation has not found its way into everyday clinical life. The common approach is to use as narrow a continuous spectrum as possible, which is accomplished partly by absorption filters. Thick filters are extremely useful for this purpose, but are limited by the required increase in tube load.

In this work we pursue another approach. We use an ordinary X-ray tube, a highly oriented pyrolytic graphite (HOPG) mirror, and an exit slit defining the Bragg angle for the desired energy and serving as a virtual source. This arrangement forms a fan beam source. The slit width can be adjusted to tune the spatial resolution. Together with a linear detector we have a slot-scan system. Some advantages of this approach have been already demonstrated by Diekmann et al.⁴.

2. METHOD

The X-ray system for monochromatic imaging was composed as follows: The basic system was a Siemens Mammomat[®] 300 mammography device, contributing the X-ray tube, the high voltage generator, the operating console, and the mechanical setup. The tube had a molybdenum anode and was operated with 35 kV voltage and 100 mA current in most cases. A permanent pre-filtration of 30 μm Mo was used.

The monochromator module (IfG - Institute for Scientific Instruments GmbH, Berlin, Germany) consisted of a 2 cm x 5 cm HOPG crystal (Optigraph, Berlin, Germany) with a curvature radius of 480 mm and a mosaicity of 0.4°. It was mounted under the Bragg angle of 6° close to an adjustable collimator slit (Fig. 1).

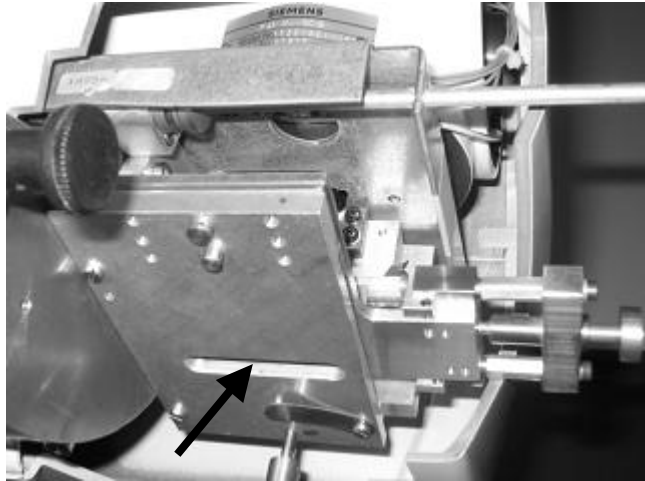


Figure 1: Monochromator mounted below the X-ray tube of the Siemens Mammomat[®] 300. The arrow indicates the collimator slit.



Figure 2: Mammography system with linear array detector (arrow) and sample carriage.

The detector was a linear array CCD detector (TH9570 by Thales Electron Devices, Moirans, France) with 4092 x 200 pixels 54 μm in size, operating in time-delayed integration (TDI) mode and delivering 12 bit digitized data. A pixel size of 27 μm is also available. The CCD was coupled to a 200 μm thick CsI scintillator layer. The performance of the detector was described by Tesic et al⁵. Since the mechanical setup could not be pivoted at this stage of investigation, the objects to be studied were moved through the X-ray beam on a stepper-motor-driven, computer-controlled carriage (Fig. 2). Details have been published elsewhere⁶.

In the case of polychromatic exposure, additional 5 mm, 10 mm, or 20 mm thick polymethylmetacrylate (PMMA) filters were applied.

The modulation transfer function (MTF) was determined from images of a lead bar phantom. This phantom (Type 40 manufactured by Hüttner) had groups of lines ranging from 0.05 mm^{-1} to 10 mm^{-1} and was positioned either almost in the scan direction or almost in the detector direction (a few degrees deviation from scan or detector direction is necessary to produce oversampling). The resulting contrast was then converted to the MTF according to the standard procedure defined in IEC 62220-1.

Homogeneously exposed images were used to determine the noise power spectra. Together with the MTF, they allowed the detective quantum efficiency (DQE) to finally be derived. Details are explained in the Handbook of Medical Imaging⁷.

Furthermore, in this study we investigated the signal-difference-to-noise ratio (SDNR) of different materials under monochromatic compared to polychromatic radiation. The SDNR is a well-suited quantity to characterize the contrast behavior of an object, since it is invariant to many image-processing operations, e.g. windowing. As a figure of merit we chose SDNR^2/K with the air kerma K at the surface of the phantom, because this variable allows results derived from different measurements to be easily compared.

In addition, we imaged a contrast detail phantom (CD-MAM, University of Nijmegen, The Netherlands) containing 410 gold dots of different diameters (0.1 mm to 3.2 mm) and thicknesses (0.05 μm to 1.25 μm).

3. RESULTS

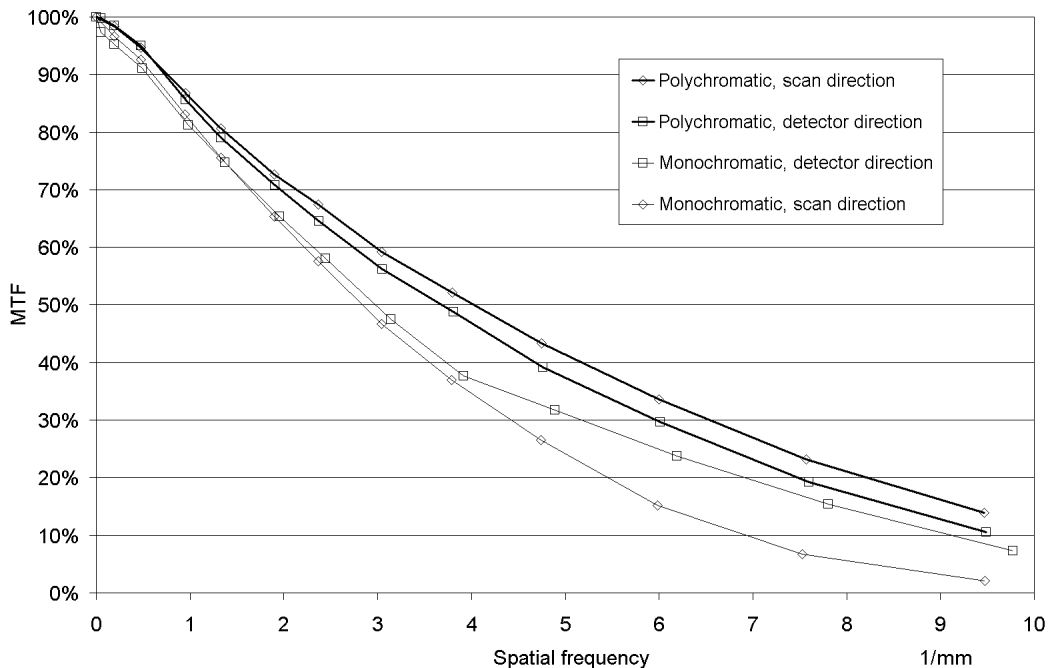


Figure 3: MTF as a function of spatial frequency, measured in detector and scan direction with monochromatic or polychromatic radiation, respectively.

Fig. 3 shows the MTF as a function of spatial frequency. The MTF extends nearly to 10 mm^{-1} which can be expected from the $54 \mu\text{m}$ pixel size (Nyquist frequency 9.3 mm^{-1}).

Using monochromatic radiation, the resulting MTF is somewhat lower than in the polychromatic case. This can be explained by the beam pathway and the fact that the polychromatic X-rays are emitted from a well-defined focus point resulting in a sharp image. The monochromatic X-rays must have been reflected by the HOPG crystal which consists of numerous crystallites with a mosaicity of 0.4° . This results in a blurring of the virtual focus and finally to a lower spatial resolution. The spatial resolution can be increased by reducing the exit slit width, which, however, would reduce the X-ray intensity.

An additional effect arises from magnification which depends on the focus – detector distance. The polychromatic radiation comes directly from the focus and projects onto the detector a magnified image of the lead bar pattern, which is located about 3 cm above the detector. The monochromatic X-rays are gained by Bragg reflection from the curved HOPG surface. Therefore, in scan direction the slit serves as an X-ray source. It is closer to the detector and the phantom than the tube focus. Therefore, the lead bar pattern becomes more magnified, which can be seen from the resulting measuring points that are shifted to somewhat lower frequencies. Since the slit is wider than the tube focus, the resulting MTF is rather low. In detector direction the HOPG is flat and the X-rays can penetrate the whole length of the slit. This leads to a beam which is rather diffuse. Consequently, a low-frequency drop in the MTF can be observed. The measuring points are shifted to higher frequencies, i.e. the X-rays seem to emerge from a more distant source. This effect has still to be investigated in more detail.

Homogeneously exposed images were used to determine the noise power spectra. In the polychromatic case, one image was taken with a dose of 1.48 mGy. The dose that could be delivered through the monochromator was only $102 \mu\text{Gy}$. Therefore, 16 images were summed up to gain a total dose of 1.632 mGy. The DQE was then calculated along the axes and in a diagonal direction. Since the system properties are nearly isotropic in the polychromatic case, only the diagonal DQE is plotted in Fig. 4. The dependence of the DQE on orientation under monochromatic conditions reflects the properties of the MTF discussed above.

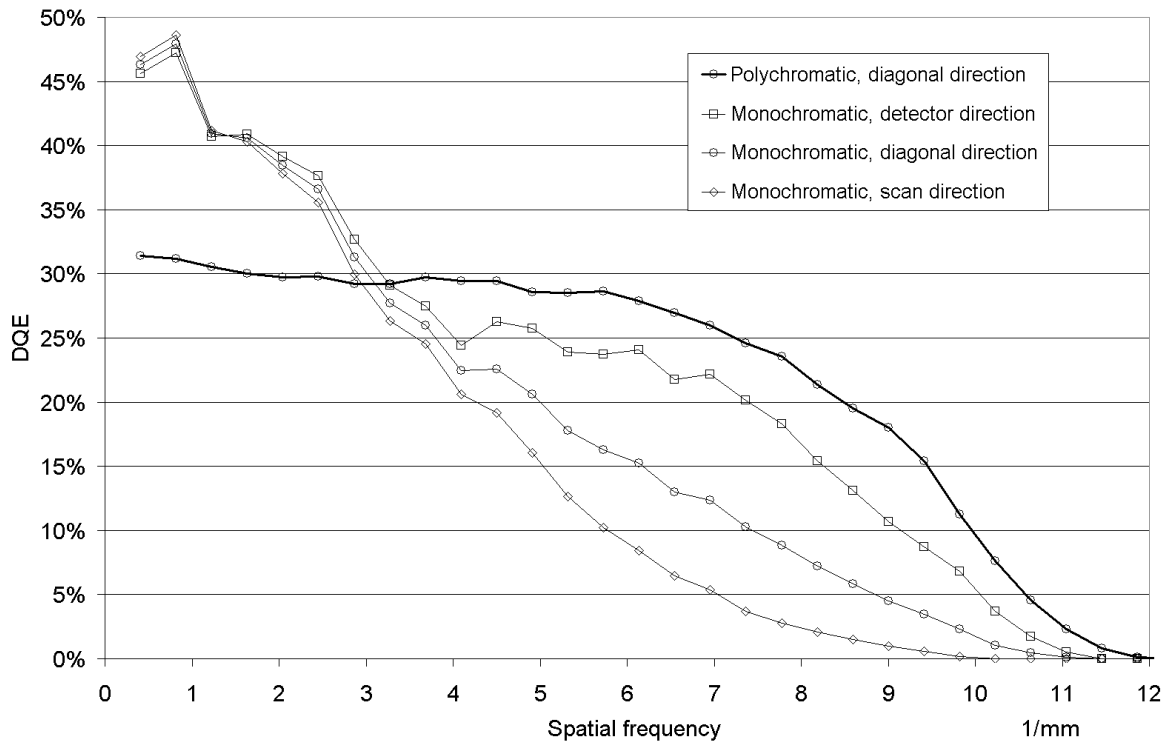


Figure 4: DQE as a function of spatial frequency, measured in detector and scan direction with monochromatic or polychromatic radiation, respectively. Plots in diagonal direction are an average between detector and scan direction.

The higher DQE at lower spatial frequencies, i.e. below 3 mm^{-1} , for monochromatic compared to polychromatic radiation can be explained by the fact that the absorption of the incident 17.5 keV X-ray quanta is higher than for the spectrum used which extends up to 35 keV.

The contrast measurements mentioned above were performed on a series of four metal foils (Al, Cu, Y, and Ag), whereas the metals are characterized by their different K-edge energies. The sample parameters are listed in Table 1. The first metals (Al, Cu, and Y) have a K-edge with an energy below the monochromatic energy of 17.5 keV while the Ag K-edge is above. Ca as a constituent of calcifications and bones, I and Gd as the major contrast media, and Au used in the CD-MAM phantom are also listed for comparison.

Table 1

Metal	Thickness	Mass density	Atomic number Z	K-edge energy
Al	500 μm	2.70 g/cm^3	13	1.56 keV
Ca		1.54 g/cm^3	20	4.04 keV
Cu	25 μm	8.92 g/cm^3	29	8.98 keV
Y	25 μm	4.47 g/cm^3	39	17.04 keV
Ag	25 μm	10.49 g/cm^3	47	25.51 keV
I		4.94 g/cm^3	53	33.17 keV
Gd		7.89 g/cm^3	64	50.24 keV
Au	0.4 μm	19.32 g/cm^3	79	80.72 keV

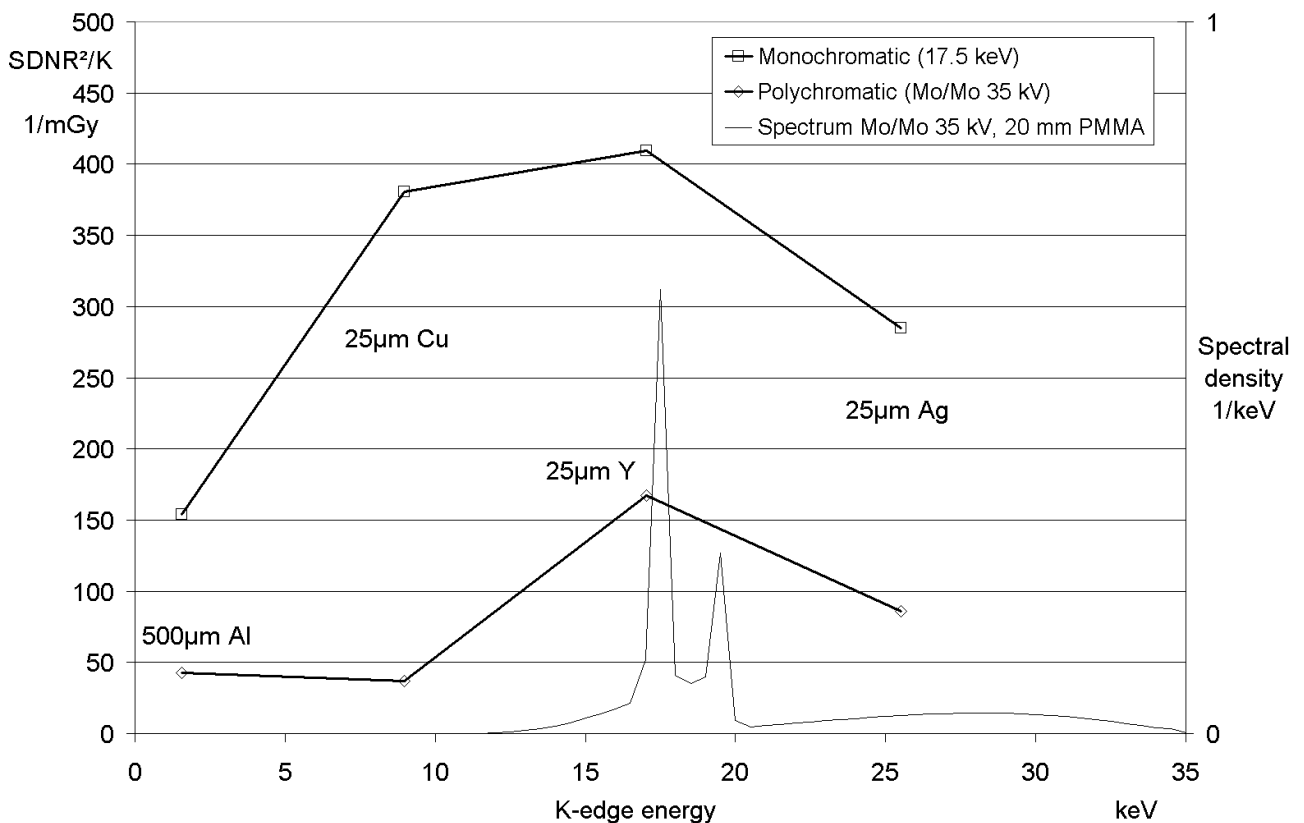


Figure 5: SDNR²/K for materials of different K-edge energy, measured with monochromatic or polychromatic radiation, respectively (left scale). The polychromatic spectrum is shown for comparison (right scale).

The results can be seen in Fig. 5. Since the metal foils are very different in thickness and density, the absolute values of $SDNR^2/K$ span a wide range. The important feature is the enhancement in $SDNR^2/K$ under monochromatic conditions by a factor of 2.5 to 10.

Fig. 5 demonstrates the enormous advantage of monochromatic exposure in visualizing low contrast details compared to ordinary polychromatic spectra.

The CD-MAM phantom imaged with polychromatic radiation and additional 20 mm PMMA is shown in Fig. 6. In particular, the dots with a gold thickness above $0.1 \mu\text{m}$ are fairly visible. Fig. 7a and Fig. 7b show some details of CD-MAM phantom images taken under polychromatic and monochromatic conditions, respectively.

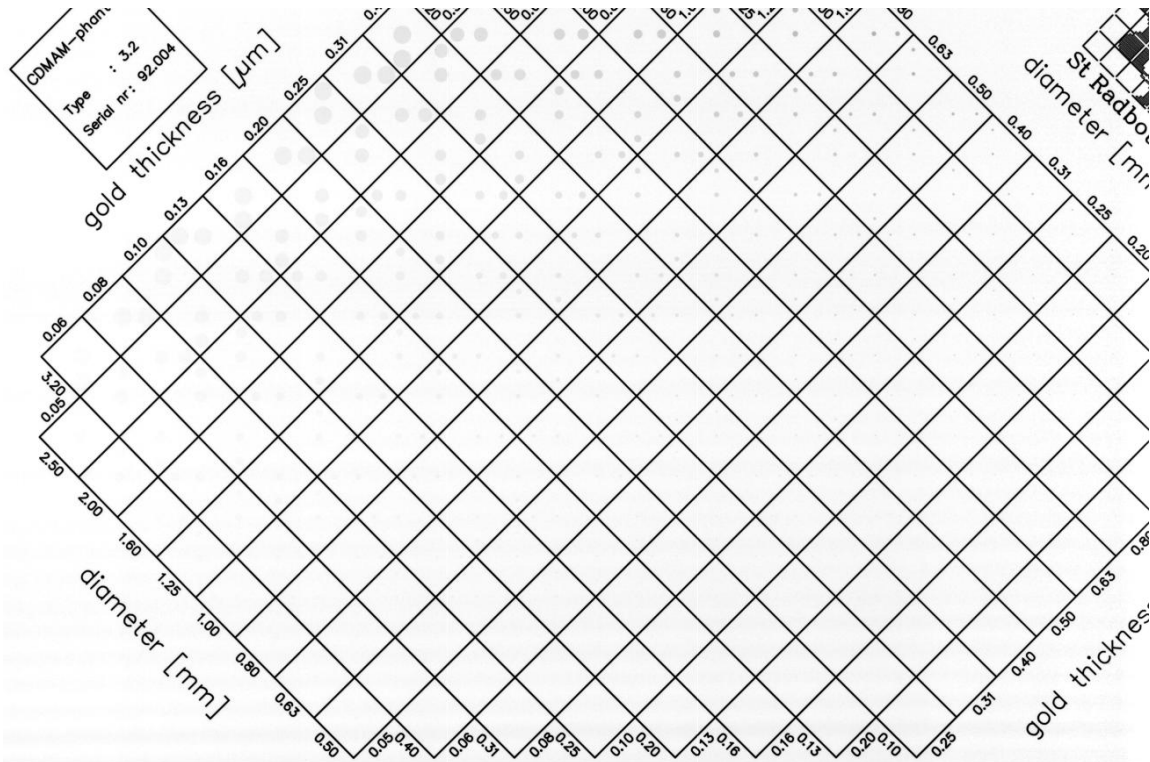


Figure 6: CD-MAM phantom imaged with polychromatic radiation.

In Fig. 7b a certain contrast enhancement can be seen over Fig. 7a which demonstrates the superiority of monochromatic imaging. Nevertheless one should consider that the images shown here underwent windowing which makes assessment difficult. Moreover, Fig. 7b is rather noisy although nine images were added up to compensate for the low dose in the monochromatic images. However, the dose in the monochromatic case (Fig. 7b) still remains lower than in the polychromatic case by a factor of two (Fig. 7a). Therefore, a further quantitative evaluation is necessary.

Since it is difficult to compare $SDNR$ s of samples of very unequal thickness (e.g. $0.4 \mu\text{m}$ Au and $500 \mu\text{m}$ Al), the $SDNR^2/K$ of $1\text{-}\mu\text{m}$ -thick layers was calculated for all materials and shown in Fig. 8. In the monochromatic case, the measured absorption was reduced according to an exponential law. In the polychromatic case, the attenuation curve of the spectrum was used. In the case of Ca, I, and Gd, where no measurements had been performed, simulated data are plotted instead.

Finally, the $SDNR^2/K$ enhancements of the monochromatic images were calculated for each material on a $1\text{-}\mu\text{m}$ -layer basis. Fig. 9 shows the results. The strongest enhancement of $SDNR^2/K$ can be obtained with Cu and Y. Even low concentrations of these materials will result in a considerable $SDNR$ at low X-ray doses. Therefore, these materials seem to be particularly suitable for new contrast media if an X-ray system with a monochromatic radiation source is available.



Figure 7a: Details of the CD-MAM phantom imaged with polychromatic radiation.

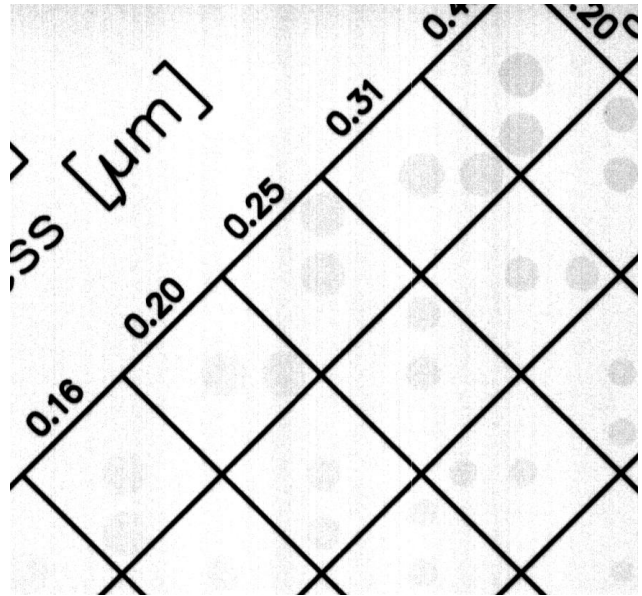


Figure 7b: Details of the CD-MAM phantom imaged with monochromatic radiation.

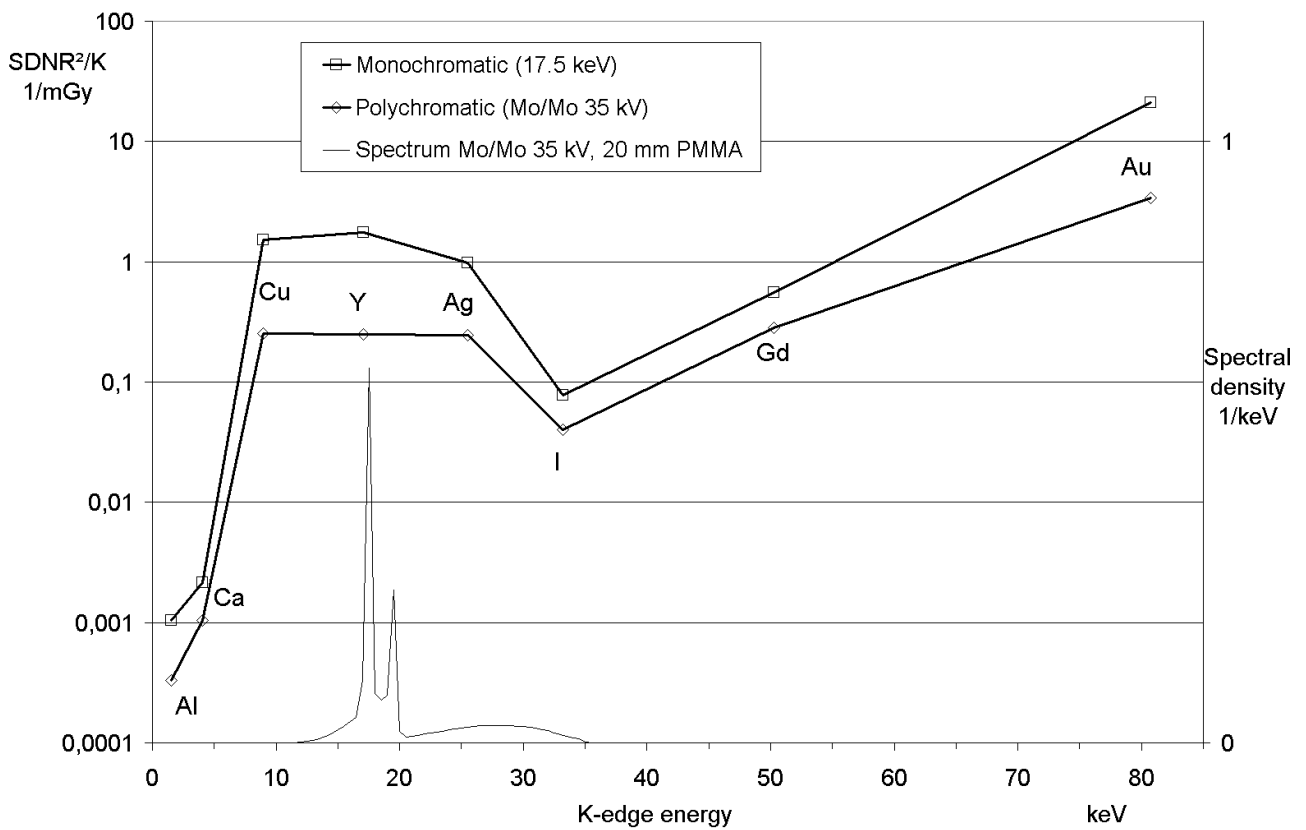


Figure 8: SDNR²/K for materials of different K-edge energy, measured with monochromatic or polychromatic radiation, respectively, and normalized to a material thickness of 1 μm (left scale). Ca, I, and Gd data are simulation results. The polychromatic spectrum is shown for comparison (right scale).

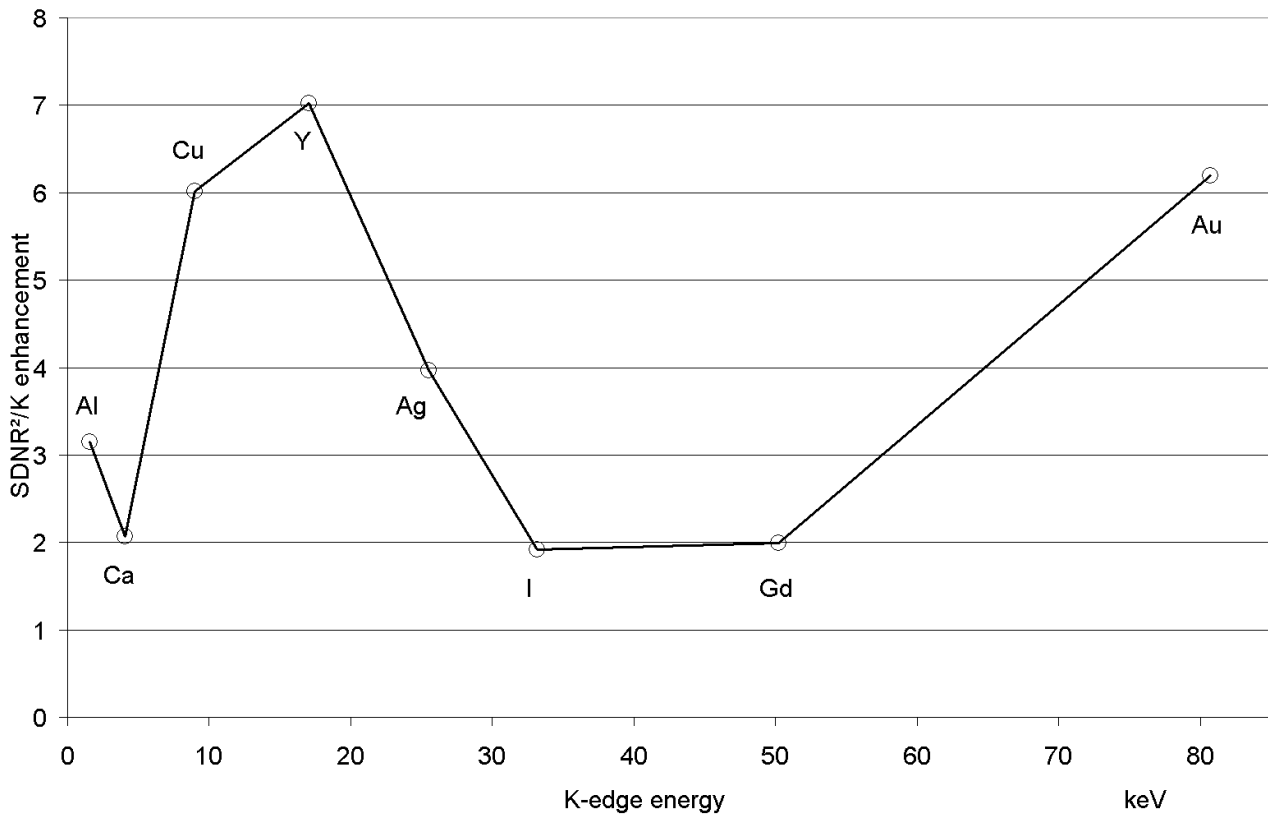


Figure 9: SDNR²/K enhancement of monochromatic over polychromatic images for materials of different K-edge energy and 1- μ m thickness (left scale).

4. CONCLUSIONS

In this study we investigated some possibilities of monochromatic X-rays in medical diagnostic applications. The main point is that we are dealing with a system which does not need a synchrotron. The monochromator module proposed here consisting of a curved HOPG crystal in combination with a collimator slit is easy to install and cost-effective. Admittedly, only a slot-scan system can be realized. This comes with all the well-known disadvantages of scanning systems, particularly the long scanning time and the high tube load.

The dose delivered by the arrangement with a monochromator and a slit is by a factor of about 20 lower than in the conventional case. To gain images with an equivalent quantum noise, the exposure in the monochromatic case should be comparable to the polychromatic case. That would necessitate either much stronger X-ray tubes or largely extended exposure times. In our experiments, we repeated the scans several times and added up the single images to obtain a virtual high-dose image. This is not feasible for routine diagnostic procedures since the total time necessary to obtain an image would be far too high.

One solution to overcome these obstacles would be much higher tube power. Such tubes are not available at the moment. Another solution could be an arrangement with multiple mirrors and slits which might allow a larger sample area to be exposed at one time. This field is still open for further investigations.

The 54- μ m pixel detector used in our setup should be able to deliver good spatial resolution. Fig. 3 showed that in the polychromatic case the MTF does not achieve the excellent values that can be obtained with a 70- μ m-pixel selenium-based detector⁸. This can be explained by the light propagation inside the CsI scintillator on the CCD. The loss in MTF especially at higher frequencies in the monochromatic case compared to the polychromatic one can be attributed to the

increase of the effective source size due to the mosaicity of the HOPG crystal. The slot-scan geometry also plays an important role. It leads to different virtual positions of the imaging focus depending on scan direction. If very high spatial resolution with such a system is required, additional efforts would be necessary to improve the MTF.

The DQE could certainly be higher if the absorber were improved, i.e. a thicker scintillator would absorb the incident radiation more effectively. This would also reduce the tube load problems mentioned above. The anisotropy of the DQE in the monochromatic case reflects the features of the MTF already discussed.

One aim of this work was to work out the advantages of monochromatic X-rays for contrast enhancement. Fig. 5 and Fig. 9 nicely illustrate how different materials can be used to gain more contrast, i.e. a higher SDNR. The advantage of the current setup in terms of contrast enhancement for monochromatic compared to polychromatic X-rays could thus clearly be demonstrated. This contrast enhancement improves the diagnostic value for existing, iodine-based contrast media and can also support the development of new dedicated contrast agents. Whether this contrast enhancement will also be experimentally verified in the detection of micro-calcifications will be a task for further studies. Based on the promising contrast enhancement for calcium calculated in Fig. 8 and Fig. 9, these studies are necessary.

REFERENCES

1. The system discussed in this work is not commercially available.
2. M. Säbel, H. Aichinger, "Recent developments in breast imaging", *Physics in Medicine and Biology* **41**, 315-368, 1996
3. J. M. Boone, J. A. Seibert, "A comparison of mono- and poly-energetic X-ray beam performance for radiographic and fluoroscopic imaging", *Medical Physics* **21**, 1853-1863, 1994
4. F. Diekmann, S. Diekmann, K. Richter, U. Bick, T. Fischer, R. Lawaczeck, W. R. Press, K. Schön, H. J. Weinmann, V. Arkadiev, A. Bjeoumikhov, N. Langhoff, J. Rabe, P. Roth, J. Tilgner, R. Wedell, M. Krumrey, U. Linke, G. Ulm, B. Hamm, "Near monochromatic X-rays for digital slot-scan mammography: initial findings", *European Radiology* **14**, 1641-1646, 2004
5. M. M. Tesic, M. Fischer Piccaro, B. Munier, "Full field digital mammography scanner", *European Journal of Radiology* **31**, 2-17, 1997
6. R. Lawaczeck, V. Arkadiev, F. Diekmann, M. Krumrey, "Monochromatic X-rays in digital mammography", *Investigative Radiology* **40**, 33-39, 2005
7. J. Beutel, H. L. Kundel, R. L. Van Metter, Handbook of Medical Imaging , Volume 1. Physics and Psychophysics, SPIE Press, Bellingham (WA), 2000
8. M. Hoheisel, L. Bätz, T. Mertelmeier, J. Giersch, A. Korn, "Modulation transfer function of a selenium-based digital mammography system", *IEEE Transactions on Nuclear Science*, in press